Deep Ritz Method for Uncertainty Quantification: Phase Field Fracture

Conor Rowan

Spring 2024

Contents

1 Introduction

Fracture is a phenomena which can can be very sensitive to uncertainty. This can be conceptualized as a consequence of the localized and nonlinear nature of crack formation. For example, one can reasonably imagine that crack formation does not depend continuously on material parameters. For one setting of the material parameter, a structure may exhibit stable or negligible crack growth, whereas the structure may fail catastrophically at another setting. This dramatic change in the output may be the consequence of apparently small changes

in the input material properties. Similarly, because cracks localize to very narrow bands, and often initiate around local weaknesses in the material, the nature of the crack pattern also exhibits strong sensitivity to model input parameters. These considerations demonstrate that it is both interesting and important to quantify uncertainty in the field of fracture mechanics. In this report, we use a popular and relatively recent approach to modeling damage/cracks in elastic bodies called the "phase field" model of fracture. One of the appealing characteristics of this model is that the solution for the crack pattern and elastic response of the body are the minimizers of a "total potential energy" functional, allowing the solution to be found using minimization procedures rather than solving systems of equations. The existence of this energy functional makes a Ritz method appealing, whereby the energy is discretized then minimized. This contrasts with standard Galerkin methods, for which a condition for the minimum of the energy functional is derived in a continuous sense, and then discretized. We will make use of a neural network discretization of the displacement and phase field in minimizing the energy functional, giving this the name "Deep Ritz method." This approach is potentially beneficial because the parameters of the neural network build both the shape functions and their corresponding weights, allowing more freedom to represent ac a solution with localized behavior whose position is not known a priori. The discretized solution depends nonlinearly on the parameters of the neural network unlike a traditional spectral method. However, the phase field model is inherently nonlinear, meaning that both neural network and traditional spectral discretizations require an iterative solution procedure. This could be gradient-based energy minimization or a Newton-Raphson method to solve the nonlinear system corresponding to the condition for the minimum of the energy. To be sure, the neural network introduces additional complexity into the "loss landscape" defined by the energy functional, however it does not change the essential character of the minimization problem. The logic of the Deep Ritz method is that additional complexity in the loss landscape is overshadowed by the convenience of a global discretization, and the tremendous flexibility of neural networks to represent complex and localized solution behavior. Computing the dependence of the solution on uncertain input parameters can also be accomplished by extending the Deep Ritz framework to a stochastic setting. Combining the phase field model with neural network discretizations and the stochastic form of the minimum energy principle gives rise to a very compact technique for understanding the uncertain fracture response of a structure.

2 Principle of Minimum Expected Potential Energy

To compute the dependence of the displacement and phase field on uncertain input parameters, we will make use of the fact that the minimum expectation of the potential energy associated with a partial differential equation (PDE) cor-

responds to a solution in the stochastic and physical space. This is a technique for performing uncertainty quantification on PDE's with variational principles. The more common Polynomial Chaos Expansion (PCE) relies on the stochastic Galerkin method, which computes a Galerkin optimal approximation first in the stochastic space, and then in the physical space. This is usually accomplished with a multiplicative (tensor product) decomposition of the solution's dependence on the spatial coordinate(s) and parameter(s). In our case, we will assume that that the dependence of the solution on the physical coordinates and parameters is captured with a single set of basis functions. With this setup, we can show the equivalence of the stochastic Galerkin method with the principle of minimum expected potential energy for elliptic PDE's. Consider a simple 1D boundary value problem (BVP)

$$\kappa(x,y)\frac{\partial^2 u}{\partial x^2} + f(x) = 0, \quad u(0) = u(1) = 0$$

where u is a displacement-like quantity, $x \in [0,1]$ is the spatial coordinate, and $y \in [-\infty, \infty]$ is a random parameter that determines the spatially varying material coefficient κ. Let's say that the statistics of the random parameter are described by a known density function $\rho(y)$. For simplicity, we are assuming that there is only one random parameter and one spatial dimension to ease the presentation, though the following considerations are general. Because the coefficient in the BVP depends on the parameter y, the solution u will as well. To perform uncertainty quantification, we need to understand how the solution $u(x)$ changes with the parameter y. Once we have a relationship $(x,y) \to u(x,y)$, we can compute statistical quantities of interest such as the mean and variance of the solution. We can discretize the solution in the "parameter space" of y in the same way that we discretize it in physical space. This could be done in the following way:

$$u(x,y) = \sum_i u_i(x)\Psi_i(y)$$

This is a tensor-product type decomposition analogous to how we discretize space-time PDE's, where the coefficients control the time dependence of spatial basis functions. This is how a typical Polynomial Chaos Expansion proceeds. When using neural networks to discretize a PDE, it is convenient to not distinguish between the parameters and spatial coordinates: they both influence the solution as inputs to the first layer of the network. More closely aligned with the neural network's "indifference" to parameters, we discretize the solution in physical and parameter space with a single set of basis functions:

$$u(x,y) = \sum_i u_i\Psi_i(x,y)$$

The solution $u(x,y)$ is simply some surface, and we can build it up in any way we wish. We take this approach because it is more closely aligned with how a neural network handles the spatial coordinates and parameters. The

Galerkin method must account for the fact that y is a random variable. Instead of simply integrating against each element of the basis for the displacement approximation, we use the density of y to weight contributions to the weak form by their corresponding density. This is natural if we think of the density as "prioritizing" points in parameter space which are more likely to be observed. In other words, we typically have no notion of importance for points in the spatial domain, but in the parameter space, there are some regions with zero or almost zero probability. There is no sense in weighting these equivalently in forming the residual for the weak form. More concretely, it can be seen that integrating against the density is equivalent with Galerkin optimality for the expected error of the approximation. It is hopefully clear that in the presence of randomness, we would like to minimize the expected error as opposed to an unweighted error, as the expectation operation will tend to prioritize reducing error in regions which are frequently observed. The stochastic Galerkin projection for the 1D boundary value problem yields

$$\int_0^1 \int_{-\infty}^{\infty} \left(\kappa(y) \frac{\partial^2 u}{\partial x^2} + b \right) \Psi_j \rho(y) dy dx = 0$$

Plugging in the displacement approximation, integrating by parts, and noting that $\Psi_j(0, y) = \Psi_j(1, y) = 0$ for each j, we obtain the discrete standard weak form for the stochastic PDE:

$$\sum_i u_i \left(\int_0^1 \int_{-\infty}^{\infty} \kappa(y) \frac{\partial \Psi_i}{\partial x} \frac{\partial \Psi_j}{\partial x} \rho(y) dy dx \right) - \int_0^1 \int_{-\infty}^{\infty} b \Psi_j \rho(y) dy dx = 0$$

$$\implies \sum_i u_i \langle K_{ij} \rangle - \langle F_j \rangle = 0$$

where $\langle \cdot \rangle$ indicates the expected value taken with respect to the random parameter y. The notation K_{ij} and F_j is used for the usual definition of the stiffness matrix and force vector. We know that equations like this come from the gradients of quadratic energies of the form

$$\Pi = \frac{1}{2} \langle K_{ij} \rangle u_i u_j - \langle F_i \rangle u_i$$

In this case we have expected value operations on the stiffness matrix and force vector. It can be seen by "reversing the discretization" that the continuous form of the energy functional is

$$\Pi = \int_0^1 \int_{-\infty}^{\infty} \left(\frac{1}{2} \kappa(y) \left(\frac{\partial u}{\partial x} \right)^2 \rho(y) - b u \rho(y) \right) dy dx$$

Thus, the stochastic Galerkin method applied to the strong form of the governing equations is equivalent to minimizing the expectation of the potential energy. This is analogous to the equivalence in the deterministic case between

the condition of minimal energy and the weak form of the governing equations. Thus, we see that the minimum expectation of the energy is simply a re-casting of the stochastic Galerkin method which, in our case, is especially convenient for conducting uncertainty quantification when the PDE is discretized with a neural network. The same logic can be applied to the more complicated equations for phase field fracture to show that the stochastic Galerkin method, which we think of as the "ground truth" for optimal approximations, is equivalent to the minimum of the expected energy.

3 Phase Field Fracture Model

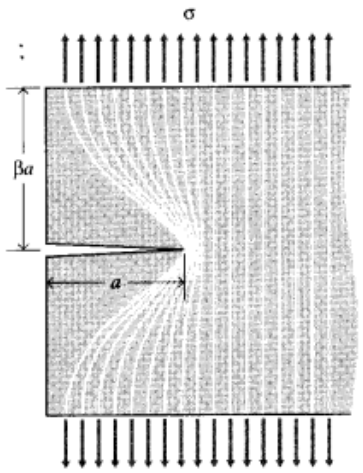

Figure 1: Two triangular regions with base a and height βa are shielded from carrying any load by the crack. The height of this region has no obvious a priori value, and is controlled by the parameter β. This parameter can be estimated by appealing to other physical considerations, but for our purposes we treat it as a given.

One might trace the origins of the phase field model of fracture back to the work of Griffith's in the early 20th century. Griffith analyzed brittle fracture of a semi-infinite plate with an existing crack of length a, as shown in Figure 1. He argued that as the crack grows, a triangular region of material unloads and becomes stress free. This corresponds to a "liberation" of strain energy from the structure. However, the crack forms by breaking atomic bonds holding the material together, and this requires energy. Thus crack formation also acts to increase the energy of the system. Assuming that the external loads do no work as the crack grows, and that the stress state outside of the triangular region is unaffected by crack growth, we can write the change in the structure's energy

as a result of crack growth as

$$\Delta U = 2\gamma\Delta a - \frac{1}{2}\sigma\epsilon\Delta A = 2\gamma\Delta a - \frac{\sigma^2}{2E}\Big((a+\Delta a)^2\beta - a^2\beta\Big)$$

where ΔA is the increase in the area shielded by the crack. The first term is the work required to form two new surfaces (one on either side of the crack), where we assume that the energy associated with crack formation is proportional to the crack length. The parameter γ is material specific and controls the resistance to crack formation. The second term is the released strain energy as a result of advancing the crack from length a to $a + \Delta a$, where the strain energy for the plate is computed using a uniaxial stress assumption, and by multiplying the energy density by the area. Expanding the above expression and neglecting the quadratic dependence on the increment in crack growth, we obtain

$$\Delta U = \Big(2\gamma - \frac{\beta\sigma^2}{E}a\Big)\Delta a$$

Griffith's argued that the crack is stable when increasing its length increases the energy of the system, i.e. $\Delta U > 0$. Alternatively, unstable crack growth occurs when increasing the crack leads to a loss of energy. The transition point is when $\Delta U = 0$, which gives a condition for the crack being at a critical point

$$2\gamma = \frac{\beta\sigma^2}{E}a$$

This equation can be used to determine determine the critical stress for a given crack length, or critical crack length for a given stress. Basically, Griffith's analysis states that cracks grow when it is energetically favorable to do so. The phase field model of fracture takes this insight and translates it into a computational framework. Inspired by continuum damage models, we introduce a damage (or phase field) variable $\phi \in [0, 1]$ which continuously interpolates between a state of undamaged material ($\phi = 0$) and fully fractured material ($\phi = 1$). This is a definition. Analogous to Griffith's approach, we can model the liberation of strain energy as a result of cracking by computing the stored strain energy of the structure as

$$\mathcal{E}_u = \int_\Omega (\phi - 1)^2 \Psi d\Omega$$

where $\Psi = \frac{1}{2}\sigma_{ij}\epsilon_{ij}$ is the usual elastic strain energy density and Ω defines the volume of the structure. Note that the function $g(\phi) = (\phi-1)^2$ satisfies $g(1) = 0$ and $g(0) = 1$. This means that undamaged material experiences no reduction in strain energy, and fully fractured material stores no energy. At intermediate values, there is a continuous reduction in the storage of strain energy at each point in the structure. This is analogous to the Griffith's model. There are other choices for what we call the "degradation function" $g(\phi)$, but we will stick with the form given above. In other words, this quadratic form is more-or-less arbitrary thought it has certain desirable properties. This expression states that damage acts to degrade the stored strain energy at each point in the structure.

Griffith's wrote *the change in energy* of the system as a competition between energy released due to crack formation and energy required to form cracks, using this to find a condition for crack stability. In the phase field model, we will write the total energy of the system in terms of an unknown displacement $u(x)$ and crack pattern $\phi(x)$. We have already written the total stored strain energy of the potentially damaged structure. The insight of this model is that the displacement and phase field should be such that the total energy is at a minimum. Whereas Griffith's model assumed a pre-existing crack, simple geometry, a given direction of crack propagation, and did not model stable crack growth, the phase field model will apply to arbitrarily complex geometries, and it will model the formation and growth of cracks. Like the Griffith's model, we expect that when the loads are small, it is "energetically favorable" to store energy in the form of strain. This is because there are serious "overhead" energy requirements to open up any cracks, controlled by a material parameter like γ. But at some point, it will be energetically "worth it" to open cracks in order to release strain energy. *The phase field model is essentially a way of quantifying that energy can be stored either through strain or through cracks, and the state of the system we actually observe is the one which minimizes the total energy.* Having seen the mechanism of strain energy storage, and having motivated the intentions of this model, we can now specify the way in which energy is stored in cracks. This energy is computed using the damage field $\phi(x)$. This turns out to be where the real artistry of the model comes into play. The first thing we do is define a new constitutive parameter $G \geq 2\gamma$ which measures the material's resistance to fracture accounting not just for the work required to break atomic bonds, but also localized plastic flow in the vicinity of the crack tip. For a crack of area Γ, the energy associated with fracture is then $G\Gamma$. The point here is that only accounting for broken atomic bonds underestimates the energy dissipated in the opening of a crack.

We need a volumetric representation of the presence of cracks, so that we can monitor the formation of damage at every point in the structure. Analogous to a strain energy density, we want a "crack density" d such that the total stored energy associated with crack formation is

$$\mathcal{E}_\phi = \int G d(\phi) d\Omega$$

This requires that cracks cannot be represented by bands of damage with zero width, otherwise we are integrating a field of measure zero. When the damage localizes to zero-width bands, the structure could be fully fractured with no energy associated with crack formation. Thus, cracks need to be smeared out over some finite width in order for the crack density approach to work. Why not simply use $\gamma(\phi) = \frac{1}{2}G\phi^2$, meaning that the total energy associated with damage is just the sum of all the local stored energies? This is a reasonable thought, but nothing prevents this from localizing to zero measure bands which cause the structure to fail to carry loads without any associated cost of crack growth. We

need to select a crack density functional which gives rise to localized, but finite width-cracks. It turns out that the following energy functional accomplishes this

$$\gamma = \frac{1}{2\ell}\left(\phi^2 + \ell^2 \frac{\partial \phi}{\partial x_i}\frac{\partial \phi}{\partial x_i}\right)$$

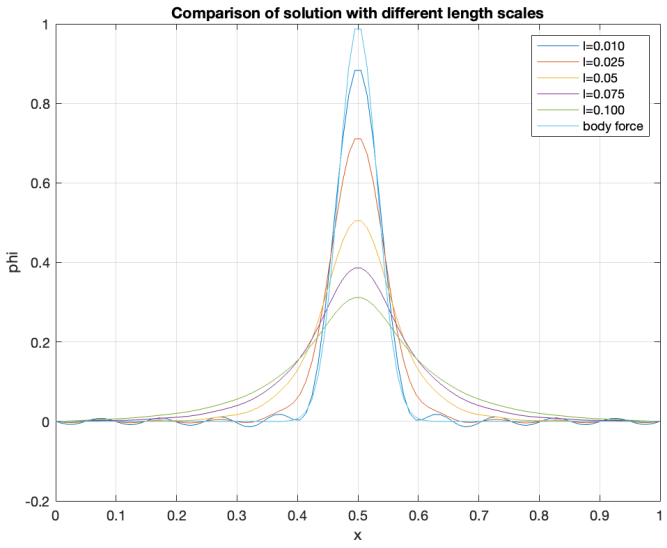

Figure 2: The length scale dictates how localized the crack is. When the length scale is large, gradients of the damage are penalized more heavily leading to more diffuse crack patterns. The damage pattern is a smeared out version of the body force as a result of the gradients in the energy functional. This solution is obtained using spectral basis functions with zero boundaries.

It is as if we added a penalty on the gradients of the damage ϕ which incur a cost for localization where gradients are large. Both the formation of the crack and its "sharpness" incur an energetic cost. This causes the crack to spread out over a finite width. The parameter ℓ is called the "length scale" and it controls how much gradients of the damage are penalized. We can think of this as scaling a diffusion-like term. Given this diffusion behavior, we do not expect the crack to be more localized than the force that drives its formation. In other words, the length scale parameter will control how much the driving force is smeared out in the formation of the crack. See the Appendix for further exploration of this crack density function. To get a feel for how this functional works in practice, we can compute its minimum, as we will do as part of solution to the phase field model. But first, we need to add a volumetric driving force term. For now, we can think of the elastic deformation of the body driving the formation of cracks in some unknown way. The energy stored in crack formation is

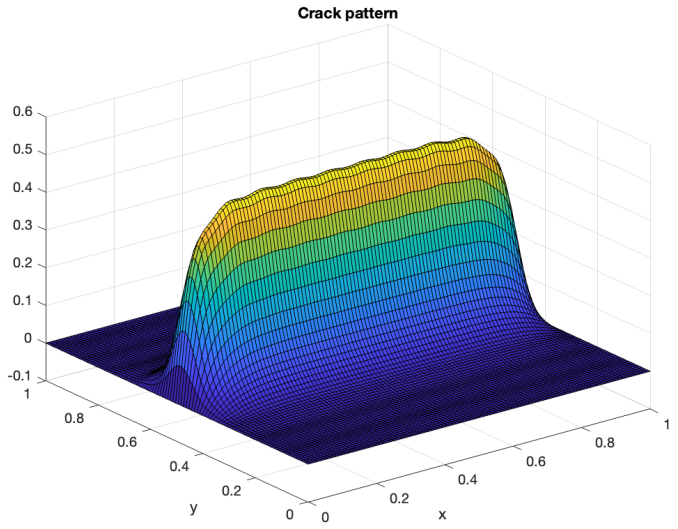

Figure 3: Two dimensional crack pattern obtained from minimizing the crack energy functional. The body force is a narrow Gaussian bump along $y = 1/2$. This solution is obtained using spectral basis functions with zero boundaries.

$$\Pi_\phi = \int \frac{G}{2\ell}\left(\phi^2 + \ell^2 \frac{\partial \phi}{\partial x_i}\frac{\partial \phi}{\partial x_i}\right) - F\phi dx$$

For our purposes, we treat the volumetric "crack-driving force" F as known. We are ignoring the part of the phase field model which involves the displacement in order to explore the behavior of the crack density functional. We want to see the kind of crack patterns the chosen density functional gives. The minimum of this functional is given by

$$\delta\Pi_\phi = \int \frac{G}{\ell}\left(\phi\delta\phi + \ell^2 \frac{\partial \phi}{\partial x_i}\frac{\partial \delta\phi}{\partial x_i}\right) - F\delta\phi dx$$

With standard methods, we discretize the displacement in terms of a set of basis functions f_j, meaning that $\phi = \sum_j \phi_j f_j$. The variation $\delta\phi$ is discretized with same set of basis functions. Noting that the variation is arbitrary, we obtain a linear system for the phase field coefficients:

$$\left(\int \frac{G}{\ell}\left(f_i f_j + \ell^2 \frac{\partial f_i}{\partial x_k}\frac{\partial f_j}{\partial x_k}\right)dx\right)\phi_j = \int F f_i dx$$

See Figures 2 and 3 for some example solutions of the crack problem. This crack density functional leads to localized crack patterns which are zero outside regions where the driving force is large. The size of the length scale dictates

how localized the solution is. We see from these results that this choice of crack density will encourage the formation of narrow bands of damage as we expect from actual fracture phenomena.

Having justified this choice of crack density, we can now write the total stored energy of the system as

$$U = \int_\Omega (\phi - 1)^2 \Psi + \frac{G}{2\ell}\left(\phi^2 + \ell^2 \frac{\partial \phi}{\partial x_i}\frac{\partial \phi}{\partial x_i}\right) d\Omega$$

This is quite similar to the Griffith's model. The first term in the energy gauges how energy is stored in the form of strain, and released as a result of crack growth unloading material. The second term quantifies how energy is absorbed in the formation of cracks. Now, we know that the total potential energy functional whose minimum solves the elastic problem is the difference between the stored energy of the system and the work of external forces. This is the case for the phase field problem as well. Thus, we can finally write the energy functional which governs the phase field problem as

$$\Pi = \int_\Omega (\phi - 1)^2 \Psi + \frac{G}{2\ell}\left(\phi^2 + \ell^2 \frac{\partial \phi}{\partial x_i}\frac{\partial \phi}{\partial x_i}\right) - b_i u_i d\Omega - \int_{\partial\Omega} t_i u_i dS$$

where the external work of body forces and tractions have been subtracted from the stored energy. This is called the isotropic phase field model, because there is no distinction between what forms of strain energy drive crack growth. In one dimension, this means that compression and tension contribute equally to the formation of cracks. In higher dimensions, this means that volumetric strains drive fracture as much as strains causing distortion. We know this is not physical–tension should more readily cause fracture than compression, and we expect that a material will not yield from hydrostatic stress states. Thus, we can introduce the anisotropic phase field model, which accounts for the influence of different types of strain energy on crack formation. Conceptually, the anisotropic phase field model is a simple modification:

$$\Pi = \int_\Omega (\phi - 1)^2 \Psi^+ + \Psi^- + \frac{G}{2\ell}\left(\phi^2 + \ell^2 \frac{\partial \phi}{\partial x_i}\frac{\partial \phi}{\partial x_i}\right) - b_i u_i d\Omega - \int_{\partial\Omega} t_i u_i dS$$

The strain energy has been decomposed into a "positive" part, which is released as damage forms, and a "negative" part, which is not affected by the formation of damage. This decomposition must respect $\Psi = \Psi^+ + \Psi^-$. If one were to write out the strong form of the governing equations associated with this energy functional, it would be clear that only the positive energy Ψ^+ drives crack growth. One interpretation of this is that even when the material is fully fractured, it can carry energy in the form of Ψ^-. For example, a fractured bar can still carry compressive loads. There are various ways to decompose the energy. In one dimension, it is clear that Ψ^+ is tensile strain energy, and Ψ^-

is compressive strain energy. In higher dimensions, there is more freedom in choosing the form of this decomposition. Different decompositions correspond to different constitutive assumptions about what causes fracture.

The final aspect of the phase field model we need to consider is history dependence. We imagine the formation of cracks as a process which progresses with the quasi-static application of external forces. Fracture is an inherently path-dependent phenomenon. For example, the application of a cyclic load may not bring the structure back to its initial state if cracks form. But, there is nothing at this point that prevents cracks from closing ("healing") when loads are removed. Enforcing the irreversibility of cracks is the final ingredient of the phase field model. We thus need to track the state of the structure over the entire load path in order to understand the damage that results. Even when the load is not cyclic, we imagine loading as a process which progressively forms damage. Thus, if a structure is loaded statically by external tractions $\underline{t}(\underline{x})$, the phase field model treats this loading as incremental with external tractions

$$(t_1)\underline{t}(\underline{x}) \to (t_2)\underline{t}(\underline{x}) \to \cdots \to (1)\underline{t}(\underline{x}), \quad t_1 < t_2 < \cdots < 1$$

The displacement and phase field solution under a static load are modeled as the end result of a process of monotonically increasing loads. The energy at load step k for an anisotropic phase field model is thus given by

$$\Pi^k = \int_\Omega (\phi^k - 1)^2 \Psi^+ \left(\frac{\partial \underline{u}^k}{\partial \underline{x}} \right) + \Psi^- \left(\frac{\partial \underline{u}^k}{\partial \underline{x}} \right) + \frac{G}{2\ell} \left(\phi^{2,k} + \ell^2 \frac{\partial \phi^k}{\partial x_i} \frac{\partial \phi^k}{\partial x_i} \right) d\Omega - \int_\Omega b_i^k u_i^k d\Omega - \int_{\partial\Omega} t_i^k u_i^k dS$$

The minimum of Π^k is the displacement and phase field solution at load step k. The crack irreversibility constraint can be written simply as

$$\phi^k \geq \phi^{k-1} \quad \forall x \in \Omega$$

During the ramping up of the external forces, nowhere in the domain can the crack heal. In some cases of monotonic load stepping this constraint may be met without explicit enforcement. This is certainly the case in one spatial dimension. But for a more complex structure, a crack may form and unload some previously damaged material surrounding it. This unloading could cause the unphysical reversal of damage without explicit enforcement of the constraint.

4 Neural Network Discretization and Deep Ritz Method

A fully-connected neural network is used to discretize the solution of the phase field fracture model. We will have separate networks for the displacement u and

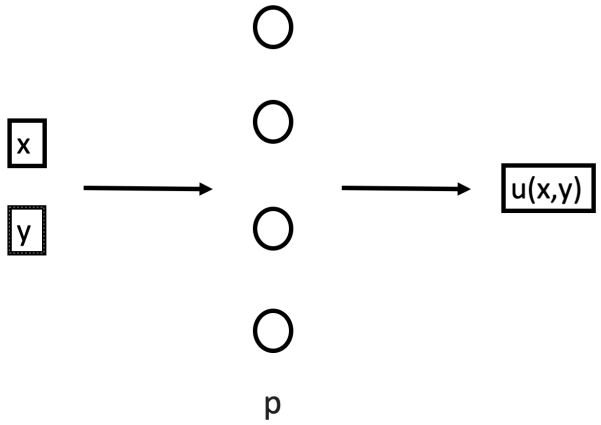

Figure 4: The spatial coordinate(s) x and parameter(s) y are inputs to a multi-layer perceptron neural network which discretizes the PDE solution $u(x, y)$. The "degrees of freedom" of the discretization are the weights and biases of the neural network, which are collected into a vector $\underline{p}$. For a given set of parameters y, the discretization describes the spatial distribution of the solution, akin to the result of a single forward solve. When we fix the spatial position x and vary the parameters y, the discretization gives us the dependence of the solution on the parameters.

phase field ϕ. In Figure 4, the neural network discretization of the displacement is shown. Both the spatial coordinate and uncertain parameters are taken in at the input layer, and are passed through a series of affine transformations and nonlinear activation steps, per the architecture of a traditional fully-connected network. The parameters $\underline{p}$ build the functional relationship between the spatial coordinate/uncertain parameter and the solution. Note that unlike a traditional discretization strategy, the solution is a nonlinear function of the parameters. Because the neural network is defined globally over physical and parameter space, it is a kind of spectral discretization. Remember that the phase field is constrained to $\phi \in [0, 1]$. This constraint can be enforced quite simply with the neural network approach. We can simply pass the output of the neural network discretizing the phase field through a function whose range is in this interval. One such example of this is

$$\phi = \frac{1}{2} \tanh\left(1 + q\tilde{\phi}(x, y; \underline{p})\right)$$

where $\tilde{\phi}$ is a fully-connected neural network for the phase field which does not necessarily respect the normalization condition. The function ϕ on the other hand respects the normalization condition by construction. The parameter q controls the sensitivity of the hyperbolic tangent to the non-normalized network

$\tilde{\phi}$. This is a hyperparameter that can be tuned for optimal performance. This is how the phase field will be discretized. No such operation is necessary for the displacement.

Using neural network discretizations of the solution, the Deep Ritz method makes use of the variational form of a partial differential equation to compute the parameters. When a PDE is variational, there is an associated "energy" functional whose minimum corresponds to a solution of the strong form of the governing equation. Not all PDE's are variational, though many problems of engineering interest such as heat conduction, linear elasticity, and nonlinear elasticity, have associated variational principles. As we have seen, this is also the case for the phase field model of fracture. A generic energy functional Π depends on the solution to the PDE through the parameters of the neural network. This can be written as

$$\Pi\Big(u(x;\underline{p})\Big) = \int_\Omega f\Big(u(x;\underline{p}), \frac{\partial u}{\partial x}(x;\underline{p})\Big) d\Omega$$

where u is the solution, $\partial u/\partial x$ is the spatial gradient, Ω is the domain over which the solution is defined, f is an "energy density," and $\underline{p}$ are the neural network parameters. Different energy densities will correspond to different physical models. Because the solution is discretized, a minimum of the energy can be computed by taking its gradient with respect to the neural network parameters. This reads

$$\frac{\partial \Pi}{\partial p_j} = \int_\Omega \frac{\partial f}{\partial u}\frac{\partial u}{\partial p_j} + \frac{\partial f}{\partial(\frac{\partial u}{\partial x})}\frac{\partial^2 u}{\partial x \partial p_j} d\Omega = 0$$

This is a system of nonlinear equations, even when the underlying physical model is linear. This is because the $\partial u/\partial p_j$ is the gradient of a neural network with respect to its parameters, which is a nonlinear function. This contrasts with traditional spectral or finite element discretizations, which lead to linear systems for linear PDE's. When treated as a system of equations, this corresponds to the weak form of the governing equations, where $\partial u/\partial p_j$ are the test functions. Due to its nonlinearity, the neural network approximates the solution on a manifold, and this nonlinear test function is a local tangent. This is Galerkin orthogonality for a nonlinear solution approximation: the PDE residual is orthogonal to the local tangent of the approximation space. Instead of explicitly solving the nonlinear system of equations, we can use the fact the system expresses a condition for a minimum and use the gradient as a search direction in an optimization framework. This avoids computing higher derivatives of the system, which would be required to form the Jacobian matrix in a Newton-Raphson method, for example. Thus, we compute the parameters such that the energy takes on a minimum, where the gradient is used as a search direction at each step in the optimization.

5 Code Verification

It can be shown that strong form of the governing equations for the 1D isotropic phase field model are

$$\frac{\partial}{\partial x}\left((\phi-1)^2 E\frac{\partial u}{\partial x}\right)+b=0$$

$$\frac{G}{\ell}\left(\phi-\ell^2\frac{\partial^2\phi}{\partial x^2}\right)=(1-\phi)E\left(\frac{\partial u}{\partial x}\right)^2$$

See the Appendix for the derivation. The first equation is the balance of linear momentum, and the second equation is the evolution law for crack growth. These equations are coupled, which prevents us from using a simple application of the method of manufactured solutions to verify the implementation of the Deep Ritz method. It turns out an analytical solution can be derived for a spatially homogeneous stress/damage response for a displacement-controlled problem. When the phase field is homogeneous, we have $\partial^2\phi/\partial x^2 = 0$. Looking at the crack evolution equation, this becomes

$$\frac{GE}{\ell}\phi=(1-\phi)E^2\epsilon^2$$

where we have multiplied both sides of the equation by the Young's Modulus E. This equation can be rearranged to give a relationship between the phase field and strain:

$$\phi=\frac{1}{1+\frac{G}{E\ell\epsilon^2}}$$

We can prescribe a strain by imposing a linear displacement field with a given slope. With the given displacement field, we can verify that the Deep Ritz method returns a spatially homogeneous phase field which matches the analytical value. See Figures 5-7 for results of the verification. For these three problems, we use $E = 10$ and $G = 1$. Experimenting with these problems indicates that once the phase field begins to take on larger values, the method exhibits some instability. For example, it is necessary to "load step" the phase field by initializing it with good guesses of the parameters (previously converged values for smaller strains) in order to converge to a constant for larger values of strain. Scaling back (relaxing) the gradients only partially alleviates this issue. This instability probably arises in part from the neural network struggling to represent a constant, but it does suggest that the method may be unstable at larger values of the damage. If we remove all of the degrees of freedom corresponding to the displacement, and force $u(x)$ to be exactly linear (as opposed to prescribing an end displacement), these issues do not arise, though this is not a practical remedy for future problems. The good news is that the Deep Ritz method does accurately reproduce the analytical solution of the phase field.

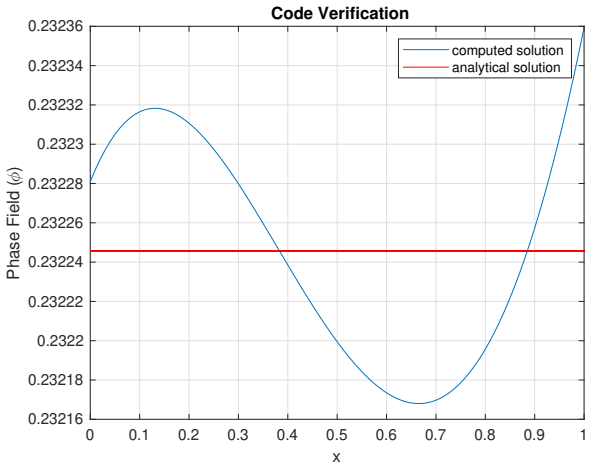

Figure 5: Displacement control is used to enforce $\epsilon = 1/2$ and the Deep Ritz method computes the phase field by minimizing the energy. We use a length scale of $\ell = 0.1$, and do not explicitly enforce $\partial^2\phi/\partial x^2 = 0$. The analytical solution is very accurately reproduced by the Deep Ritz method implementation of the isotropic phase field model. Note that here the neural network representing the displacement has to learn to represent the linear relation which arises from the prescribed end displacement.

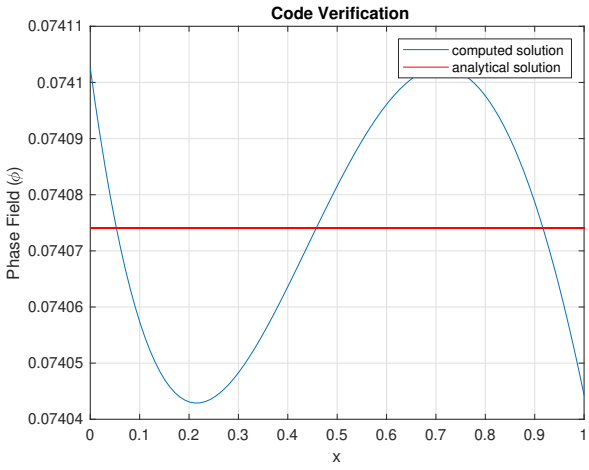

Figure 6: Displacement control is used to enforce $\epsilon = 1/5$ with $\ell = 0.2$. The computed solution accurately matches the analytical solution even when its value is small and the length scale is varied.

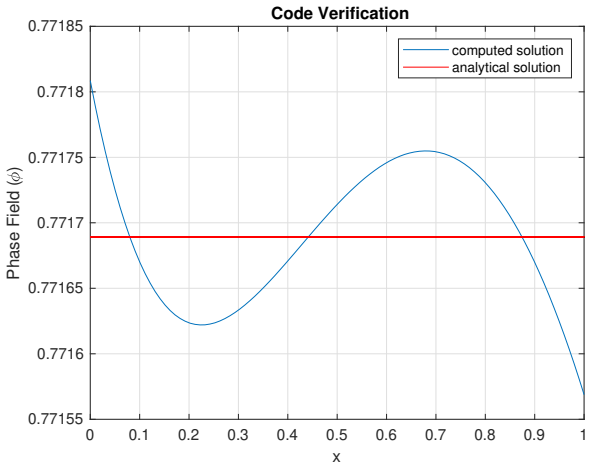

Figure 7: Displacement control is used to enforce $\epsilon = 1.3$ with $\ell = 0.2$. For large values of the phase field, the Deep Ritz method is unstable even when the gradients are aggressively relaxed. An obviously non-physical solution is obtained unless some kind of load stepping is performed, or the degrees of freedom corresponding to the displacement neural network are zeroed and a linear displacement field is enforced explicitly. The linear displacement field option is taken here. That we obtain agreement with analytical solution suggests that the phase field model is implemented correctly, but it does raise concerns about stability for more complex problems.

6 Results

Two separate neural networks are used to discretize the phase field and displacement respectively. Spatial gradients of the solution are required to form the energy, and parameter gradients are required as search directions in the optimization. The neural networks and required gradients are computed with automatic differentiation in MATLAB and written to files. A quasi-Newton optimization optimization method is used, whereby the crack irreversibility constraint is written in the form

$$g(\underline{\theta}^k) = \phi(\underline{\theta}^{k-1}) - \phi(\underline{\theta}^k) \leq 0$$

and passed into the algorithm, which can handle nonlinear inequality constraints. This contrasts with a common approach for crack irreversibility, which is to use a history variable that prevents the crack-driving force from ever decreasing. When an optimization algorithm handles constraints, it is simple to use the explicit form of irreversibility.

In this report, we only investigate 1D phase field models. Numerical experimentation with the 1D model indicated that the damage computed from

monotonic loading is unaffected by the presence of the irreversibility constraint. In other words, the solution obtained from a series of load steps with the irreversibility constraint enforced does not differ from the solution computed in a single load step. This obviates the need to repeatedly solve the energy minimization problem and frees up more computational resources for additional uncertain parameters.

For all problems under consideration, we treat the bar as loaded by a deterministic distributed force, and the material as uncertain. This set-up corresponds closely to problems of engineering interest–owing to microscale features or inherent manufacturing variation, a material is often not known deterministically, and may vary from one manufactured part to the next. Numerical experimentation indicated that the response of the phase field model is more sensitive to the fracture energy $G(x)$ than the Young's Modulus $E(x)$. Thus, the fracture energy will be a random process determined by a discrete set of uncertain input parameters. All uncertain parameters are independent and have finite support $y_i \in [0, 1]$. A "convergence tolerance" is introduced as a criteria for stopping the simulation. When the maximum change in the energy over the previous 50 optimization steps falls below this tolerance, convergence is obtained. See Table 1 for a list of parameters that are common to all of the following simulations. All optimization is performed using MATLAB's "fmincon" without any constraints and the sequential quadratic programming (sqp) algorithm. This is a quasi-Newton method which performs line searches in the direction of the gradient supplied by the objective function. In general, this method is effective when gradients are accurately computed, and might be expected in these situations to outperform a stochastic gradient method such as ADAM, which minibatches gradients and performs no line search.

Parameter	Notation	Value
Modulus	E	10
Length Scale	ℓ	0.1
Cross-sectional Area	A	1
Bar Length	L	1
Spatial Integration Points	–	100
Stochastic Integration Points	–	10-20
Distributed Force	$b(x)$	$15\sin(\pi(x - L/2))$
Parameter Marginal Density	$\rho(y)$	$-6y(y-1)$
Convergence Tolerance	–	1e-8

Table 1: Parameters for the phase field model and numerical implementation common to all simulations. Note that the number of stochastic integration points corresponds to the number of points per stochastic dimension.

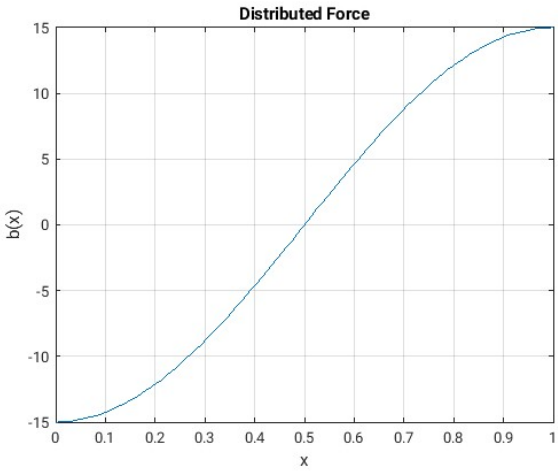

Figure 8: Distributed force driving the fracture problem of the bar.

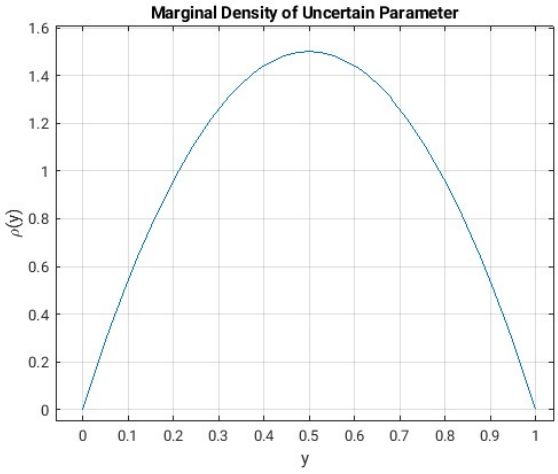

Figure 9: Marginal density function for the independent uncertain parameters. The joint probability density is computed by multiplying marginal densities as a result of the independence of the parameters. The joint density is used in computing the expectation of the energy and in Monte Carlo sampling to compute statistics of the solution.

6.1 1D Isotropic Phase Field Model with Deterministic Material

The isotropic phase field model in one spatial dimension is the simplest and will be used as a first test case. There is no distinction between tension and

compression for causing fracture and there is only one stress/strain component. Thus, the fracture strain energy is the total strain energy, i.e. $\Psi^+ = \Psi = \frac{1}{2}E\left(\frac{\partial u}{\partial x}\right)^2$, implying that $\Psi^- = 0$. The deterministic potential energy is

$$\Pi = A\int_0^L \frac{1}{2}(\phi-1)^2 E\left(\frac{\partial u}{\partial x}\right)^2 - budx - Fu(L) + A\int_0^L \frac{G}{2\ell}\left(\phi^2 + \ell^2\left(\frac{\partial \phi}{\partial x}\right)^2\right)dx$$

The bar has length L, length scale ℓ, Young's modulus E, cross-sectional area A, end force F, and fracture energy G. The problem is driven only by a distributed force, thus $F = 0$. See Figure 8 for a plot of the loading. The boundary conditions are

$$u(0) = u(1) = 0, \quad \frac{\partial \phi}{\partial x}(0) = \frac{\partial \phi}{\partial x}(1) = 0$$

where the Dirichlet boundary conditions on displacement are enforced strongly in the solution approximation, and the zero Neumann boundary conditions on the phase field are enforced weakly via the energy formulation. Using the parameters of Table 1, the energy we minimize is then

$$\Pi = \int_0^1 \frac{10}{2}(\phi-1)^2\left(\frac{\partial u}{\partial x}\right)^2 - b(x)u(x) + \frac{G}{2\ell}\left(\phi^2 + \ell^2\left(\frac{\partial \phi}{\partial x}\right)^2\right)dx$$

For the deterministic material, we will take $G = 1$. Solving the problem with the Deep Ritz method, we discretize the displacement and phase field in terms of a set of neural network parameters $\underline{\theta} = [\underline{p}_u, \underline{p}_\phi]^T$ where $\underline{p}_u$ are the parameters of the displacement neural network, and $\underline{p}_\phi$ are the parameters of the phase field neural network. The gradient of the energy with respect to the parameters is

$$\frac{\partial \Pi}{\partial \theta_j} = \int_0^1 10(\phi-1)\frac{\partial \phi}{\partial \theta_j}\left(\frac{\partial u}{\partial x}\right)^2 + 10(\phi-1)^2\frac{\partial u}{\partial x}\frac{\partial^2 u}{\partial x \partial \theta_j} - b(x)\frac{\partial u}{\partial \theta_j} + \frac{1}{\ell}\phi\frac{\partial \phi}{\partial \theta_j} + \ell\frac{\partial \phi}{\partial x}\frac{\partial^2 \phi}{\partial x \partial \theta_j}dx$$

Note that because u only depends on $\underline{p}_u$ and ϕ only depends on $\underline{p}_\phi$, the gradients with respect to the combined set of parameters $\underline{\theta}$ contain many zeros. Spatial integration is done on a uniform grid. See Figure 10 for results of the simulation, and Figure 11 for a plot of the stress in the bar.

6.2 1D Isotropic Phase Field Model with One Uncertain Parameter

We can now begin to explore the uncertainty quantification capabilities of the proposed approach. Let's assume that the fracture energy $G(x, y)$ is random

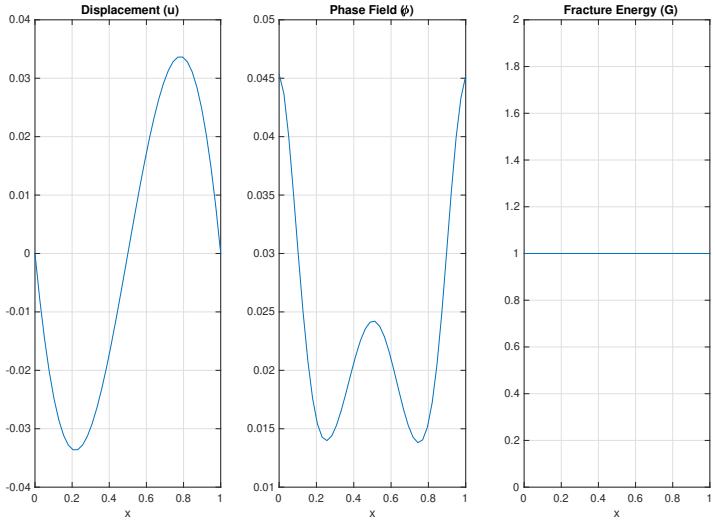

Figure 10: Converged displacement and phase field solution for the deterministic material. The shape of the displacement mirrors the distributed force, and the phase field is largest where the displacement gradients are largest. The damage takes on small values for the given body force and constant fracture energy. Note that it respects the normalization condition$\phi \in [0, 1]$ by construction. With a deterministic material, simulations take a few hundred steps to converge.

process and depending on a single parameter $y \in [0, 1]$ with probability density $\rho(y)$. The displacement and phase field pick up dependence on this parameter through the fracture energy. The expectation of the total potential energy is

$$\langle \Pi(u, \phi) \rangle = \int_0^1 \int_0^1 \left[\frac{10}{2}(\phi - 1)^2 \left(\frac{\partial u}{\partial x} \right)^2 - b(x)u \right] \rho(y) dx dy + \int_0^1 \int_0^1 \frac{G(y)}{2\ell} \left(\phi^2 + \ell^2 \left(\frac{\partial \phi}{\partial x} \right)^2 \right) \rho(y) dx dy$$

For the stochastic Deep Ritz method, we parameterize the solution fields with neural networks that take in the spatial coordinate and uncertain input, then minimize the energy in terms of their parameters. To perform the minimization, we need the gradient of the energy. The gradient of the expectation of the energy is given by

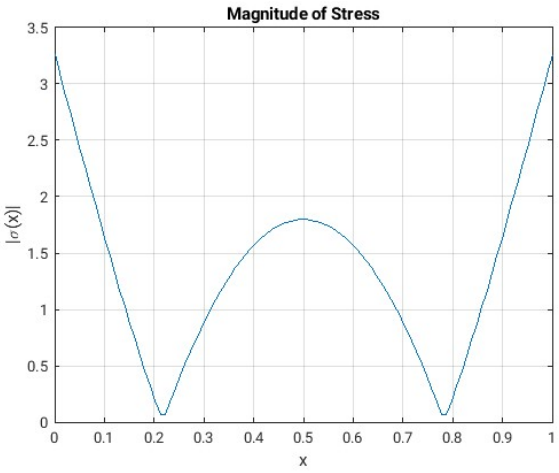

Figure 11: By comparing to the phase field solution, we see that the absolute value of the stress correlates strongly with the damage. Because we use the isotropic phase field model, there is no difference in the fracture behavior for tension and compression.

$$\frac{\partial \langle \Pi \rangle}{\partial \theta_j} = \int_0^1 \int_0^1 \left[10(\phi - 1) \frac{\partial \phi}{\partial \theta_j} \left(\frac{\partial u}{\partial x} \right)^2 + 10(\phi - 1)^2 \frac{\partial u}{\partial x} \frac{\partial^2 u}{\partial x \partial \theta_j} \right] \rho(y) dx dy$$
$$- \int_0^1 \int_0^1 \frac{\partial u}{\partial \theta_j} b(x) \rho(y) dx dy + \int_0^1 \int_0^1 \frac{G(y)}{\ell} \left(\phi \frac{\partial \phi}{\partial \theta_j} + \ell^2 \frac{\partial \phi}{\partial x} \frac{\partial^2 \phi}{\partial x \partial \theta_j} \right) \rho(y) dx dy$$

We fully integrate in the stochastic dimension to form the expected energy. This is necessary using a quasi-Newton optimization algorithm with line search. If we were to use Monte Carlo integration by sampling from $\rho(y)$ for the stochastic dimension, the line search would fail to converge because the search direction was not accurately computed. Like the spatial integration, stochastic integration is done on a uniform grid. The form of the random fracture energy is

$$G(x, y) = 1 - 0.7 e^{-200(x-y)^2}$$

See Figure 12 to visualize the dependence of the fracture energy on the random parameter. A smaller fracture energy corresponds to a smaller energetic "cost" in opening a crack, meaning that a material will more readily fracture in regions of small G. This form of fracture energy is meant to approximate a local weakness in the material whose position is random. Figure 13 shows the results of the simulation for two different settings of the random parameter controlling the fracture energy. Figure 15 shows the convergence profile for the optimization. We can use the trained neural network in order to compute statistics of the

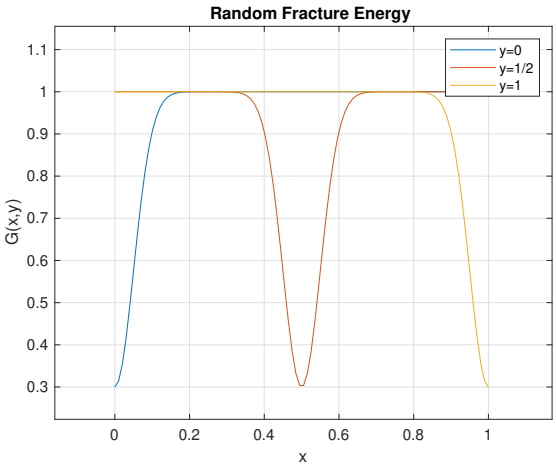

Figure 12: The fracture energy material parameter is a random process dependent on one uncertain parameter, which controls the position of the weakness along the length of the bar.

solution. We are more interested in the damage than the displacement, so this is where we focus our uncertainty quantification efforts. We can compute the pointwise mean and standard deviation of the damage by Monte Carlo sampling the trained neural network, however we first need a method to sample the distribution of the random parameter. Because the given density $\rho(y) = -6y(y-1)$ is not a standard probability distribution, we implement the inversion method to sample from this distribution. The cumulative distribution function (CDF) is

$$F(y) = \int_0^y -6\xi(\xi - 1)d\xi = -2y^3 + 3y^2$$

When we uniformly sample the CDF, the corresponding y is distributed as $\rho(y)$. We can obtain the sample of y by finding the roots of the nonlinear function

$$f(y) = -2y^3 + 3y^2 - U$$

where $U \sim \mathcal{U}[0,1]$ and $y \in [0,1]$. The $\pm$ 1 standard deviation (σ) bounds on the damage are shown in Figure 14 using $N = 1000$ Monte Carlo samples.

6.3 1D Isotropic Phase Field with Two Uncertain Parameters

When there are two independent uncertain parameters, the expectation of the energy and its gradient are

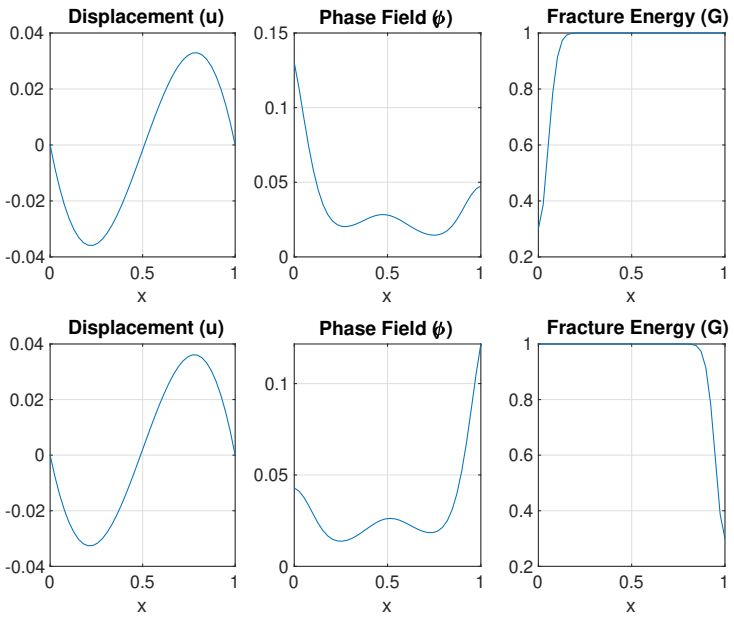

Figure 13: Results of minimizing the expectation of the total potential energy in terms of the neural network parameters. The network for both the displacement and phase field has a single hidden layer. We found that it was sufficient to have only 6 hidden units in the displacement network, and 15 in the phase field network. The displacement field is relatively insensitive to the input uncertainty, but the damage is significantly larger where the fracture energy is small. With one uncertain parameter, simulations tend to take around 1000 optimization steps to converge.

$$\langle \Pi(u,\phi) \rangle = \int_0^1 \int_0^1 \int_0^1 \left[\frac{10}{2}(\phi-1)^2 \left(\frac{\partial u}{\partial x} \right)^2 - b(x)u \right] \rho(y_1)\rho(y_2) dx dy_1 dy_2 + \int_0^1 \int_0^1 \int_0^1 \frac{G(x,y_1,y_2)}{2\ell} \left(\phi^2 + \ell^2 \left(\frac{\partial \phi}{\partial x} \right)^2 \right) \rho(y_1)\rho(y_2) dx dy_1 dy_2$$

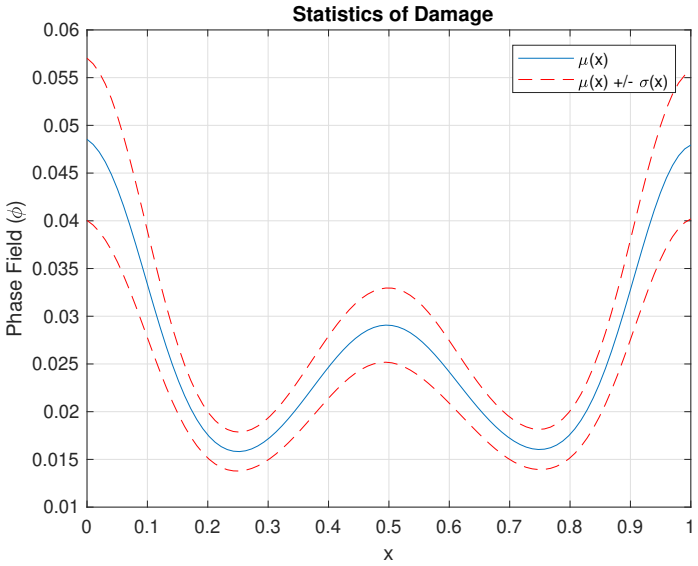

Figure 14: Pointwise mean with $\pm 1\sigma$ bounds. As expected, the uncertain damage is symmetric about $x = 1/2$, and exhibits the largest variation at the center and endpoints, where the stress is highest.

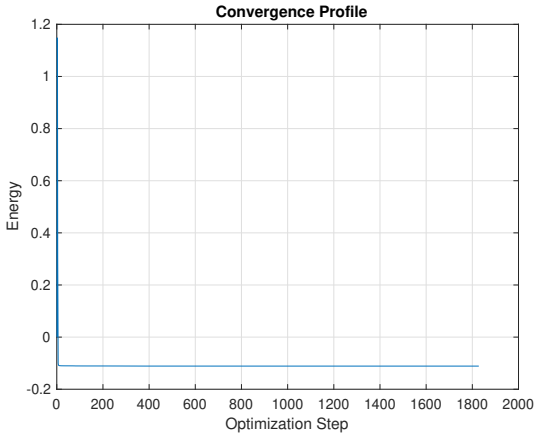

Figure 15: Convergence profile for the one parameter random fracture energy. It is not possible to use a semilog plot because the energy takes on negative values. The objective appears to be stationary after a very small number of steps, but within this region the form of the phase field is fit. It is interesting and surprising to see how insensitive the energy objective is to the phase field.

$$\frac{\partial \langle \Pi \rangle}{\partial \theta_j} = \int_0^1 \int_0^1 \int_0^1 \Bigg[10(\phi - 1) \frac{\partial \phi}{\partial \theta_j} \left(\frac{\partial u}{\partial x} \right)^2 + 10(\phi - 1)^2 \frac{\partial u}{\partial x} \frac{\partial^2 u}{\partial x \partial \theta_j} \Bigg] \rho(y_1)\rho(y_2) dx dy_1 dy_2 - \int_0^1 \int_0^1 \int_0^1 \frac{\partial u}{\partial \theta_j} b(x) \rho(y_1)\rho(y_2) dx dy_1 dy_2 + \int_0^1 \int_0^1 \int_0^1 \frac{G(x, y_1, y_2)}{\ell} \left(\phi \frac{\partial \phi}{\partial \theta_j} + \ell^2 \frac{\partial \phi}{\partial x} \frac{\partial^2 \phi}{\partial x \partial \theta_j} \right) \rho(y_1)\rho(y_2) dx dy_1 dy_2$$

The form of the uncertain fracture energy is now taken to be

$$G(x, y_1, y_2) = 1 - 0.7 y_2 e^{-200(x - y_1)^2}$$

This models a weakness of varying severity and spatial position inside the bar. The additional random parameter y_2 controls the severity of the weakness. The previous example was an extreme case of this one, where the weakness was always at the maximum severity. This form of uncertainty leads us to expect less variation in the solution arising from the two parameter fracture energy. See Figure 16 and 17 for results.

6.4 1D Isotropic Phase Field with Three Uncertain Parameters

The final case we will investigate makes use of three uncertain parameters. Already, we are reaching the limit of what we can run on a standard desktop machine in approximately an hour with the given integration grid and implementation of the phase field model. Each new stochastic dimension increases the dimension of the integration needed to form the energy and its gradient. We can not "short cut" accurately computing these quantities with mini-batching or sparse Monte Carlo integration because the line search in the optimization algorithm will not converge. Another issue is that the size of the neural network and the number of steps in the optimization required to find a minimum also increase with the number of stochastic dimensions. We will consider a material where the size, severity, and position of the weakness are all uncertain. The fracture energy is then given by three independent random parameters drawn from the same distribution:

$$G(x, y_1, y_2, y_3) = 1 - 0.7 y_2 e^{-(20 + 180 y_3)(x - y_1)^2}$$

We will not write out the energy and its gradient again. It suffices to say that we pick up an additional integral for the new uncertain parameter y_3, and the joint density of the three random parameters is $\rho(y_1)\rho(y_2)\rho(y_3)$.

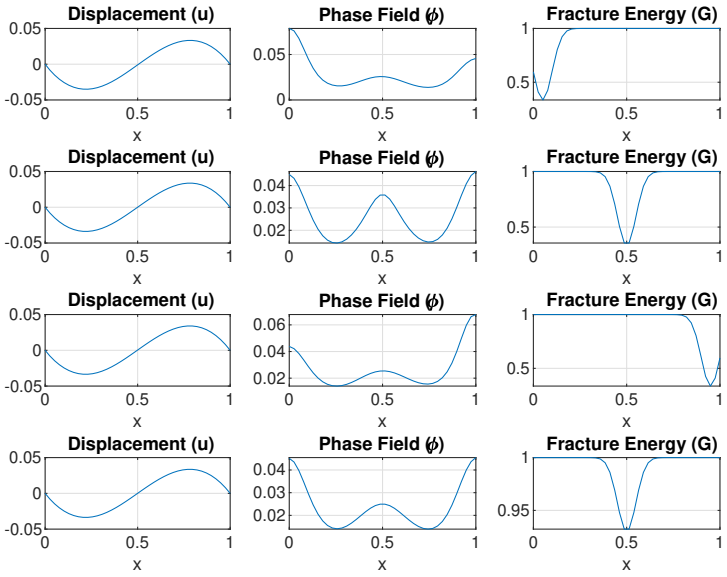

Figure 16: Converged displacement and phase field solutions at various settings of the random fracture energy. A single hidden layer network is used for both the displacement and phase field, with 6 and 18 hidden units respectively. We see that the damage is inversely proportional to the fracture energy, as expected. With two uncertain parameters, simulations tend to take approximately 2000 optimization steps to converge. This takes 10 minutes to run on a desktop machine.

7 Conclusion

We introduced uncertain parameters as additional inputs at the first layer of a neural network discretization of the displacement and phase field for a 1D fracture model. The traditional Deep Ritz method was combined with the principle of minimum expected potential energy to devise a variational method of carrying out uncertainty quantification. This method proved to be a relatively simple and elegant way to handle input uncertainties. There are a number of remaining questions/concerns at the intersection of the Deep Ritz method, phase field models, and the principle of minimum expected potential energy. These are summarized below:

- Code verification: we do not have access to a more complex analytical solution than the constant phase field case used in the "Code Verification" section. The method of manufactured solutions is not feasible for the history-dependent two field problem. Though we have observed that the

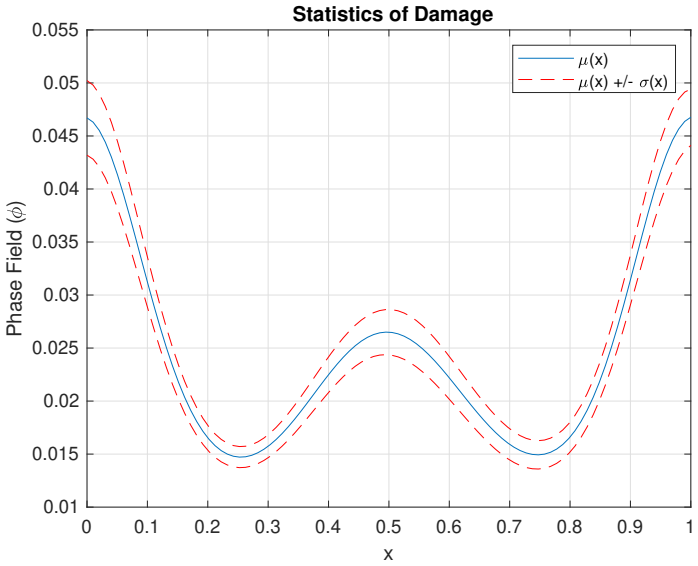

Figure 17: Uncertainty bounds on the damage for the two parameter uncertain material. The variation around the mean is smaller than in the one parameter case because the severity of the weakness, which drives variation in the value of the damage, is much smaller on average.

computed solutions reflect our intuition about what should occur, we have no more explicit guarantee than this that code is accurately solving the phase field fracture problem. For example, it was observed numerically that the bar quickly transitioned from small damage values throughout the bar ($\phi \leq 0.1$) to full fracture ($\phi = 1$). It is not clear whether this is a physically meaningful prediction of the phase field, or a numerical "instability" of the Deep Ritz method. Experimentation with the homogeneous analytical solution suggests this sudden divergence could be a numerical instability rather than a physically meaningful prediction. This explains why this report focused on load cases for which the damage stayed relatively small. It is not clear at this point how to deal with potential instabilities apart from aggressively relaxing the gradients supplied to the optimization algorithm.

- Non-deterministic solutions: the parameters of the displacement and phase field neural networks are randomly initialized every run. Even for linear physics, using a neural network discretization ensures that the energy is non-convex in the parameters. The phase field model is nonlinear and couples two different solution fields, thus we expect a complex and highly non-convex energy landscape. Experience with the MATLAB implementation demonstrated that the Deep Ritz method sometimes fails to converge

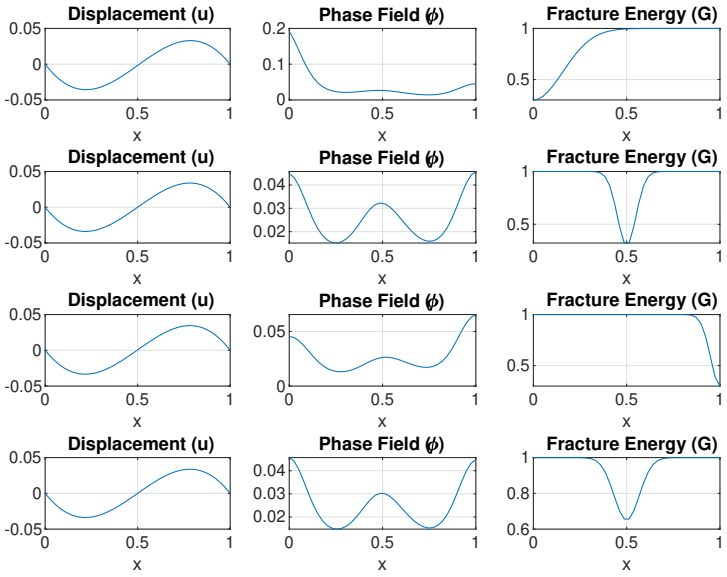

Figure 18: Displacement and phase field for a variety of settings of the fracture energy with 3 uncertain parameters. Along with its location and severity, the width of the weakness is now varied with one of the random parameters, which leads to larger values of the damage. A single hidden layer network was used for the displacement and phase field, with 6 and 18 hidden units respectively. The total run time was around 1.5 hours.

for certain initializations. Other times, we see some differences in the solutions that it converges to. These are problems if our goal is to devise a reliable numerical method for performing uncertainty quantification on the phase field model. Perhaps a better-tuned optimization algorithm can mitigate some of these issues, but this seems to be an inevitable feature of nonlinear discretizations for nonlinear problems.

- Small networks: the MATLAB implementation of the neural networks in its current form is not scaleable to large problems. We write out the neural networks for the displacement and phase field as symbolic expressions, which allows us to easily compute the spatial derivatives required for the energy objective. This method is extremely flexible and easy to implement, but is not computationally efficient. For example, when the neural network is called in the forward mode, the parameter vector which determines the weights and biases is completely "unpacked." In other words, there is not vectorized dependence of the network on the parameters, which reduces numerical efficiency. The small networks used in this report are sufficiently

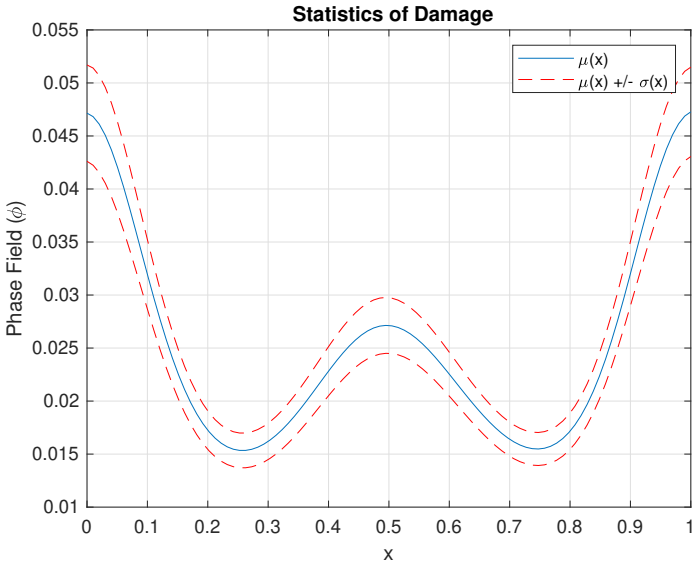

Figure 19: Uncertainty bounds on the damage for the three parameter uncertain material. We do not see the fact that much larger damage values are observed as a result of modulating the size of weakened region reflected in looking at the one standard deviation confidence interval for the damage.

expressive for the 1D problem, but this will almost certainly not be the case for higher dimensions. One upshot of the small network approach is that it suggests very deep networks are not needed, as many reports in the literature suggest. The successful application of small- to medium-sized networks could help the Deep Ritz method be competitive with traditional finite element techniques.

- Optimization algorithm: we used a quasi-Newton optimization algorithm with line search to minimize the expectation of the potential energy. Initially, this was motivated both by convenience, and a need for explicitly enforcing the irreversibility constraint between load steps. That being said, we later observed that the irreversibility constraint could be lifted in the case of 1D monotonic loading. Quasi-Newton algorithms seem to be becoming more popular in the machine learning literature, and the built-in line search is advantageous for preventing the divergence of objectives with complex loss landscapes. But the line search imposes an implicit constraint that gradients are computed accurately. This means that we could not minibatch gradients at each optimization step, and integration over the stochastic space needed to be reasonably accurate. With this constraint, the stochastic Deep Ritz method suffers from the curse of dimensionality, as every new stochastic dimension exponentially increases

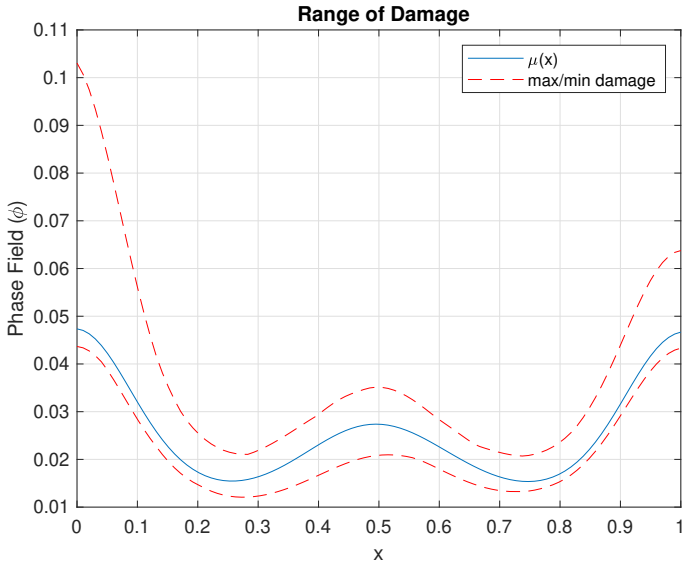

Figure 20: Largest and smallest values of the damage at each spatial point among the Monte Carlo sample from the neural network trained on the three parameter random fracture energy. It is not clear why symmetry is broken here, but the extreme cases of the parameters which give rise to larger damage values are observed with low probability and are thus not highly weighted in the energy objective.

the number of function evaluations used in computing integrals. An alternative is to use a stochastic gradient method such as ADAM, but we then lack the ability to easily tack on the irreversibility constraint to the objective. Furthermore, it is not a given that ADAM with Monte Carlo integration over the stochastic dimensions at each optimization steps outperforms the quasi-Newton method, as we expect the cost associated with allowing for inaccurate gradients is that the number of steps required for convergence is much larger.

- Load stepping/constraint: though we outlined a viable technique for load stepping and enforcing the irreversibility constraint, we did not make use of these for uncertainty quantification. If we have the ability to do constrained optimization, irreversibility presents no issues so long as it doesn't introduce convergence difficulties. But if we change optimization algorithms, it may be advantageous to reconsider the proposed technique for constraint enforcement, opting instead for something like a penalty to the energy.

- Slow convergence of the damage: in all of the cases studied in this report, it was observed that the displacement converged very early in the opti-

mization while the phase field required a much larger number of steps to find an optimal solution. A few examples indicated that the magnitude of the gradient with respect to parameter for the damage ϕ was much smaller than that of the displacement. This effect could be mitigated as a result of rescaling the material parameters E and G such that displacement and phase field contribute more equitably to the gradient. At this time, it is not clear what other techniques might be useful for expediting the convergence of the phase field.

A Crack Density Function

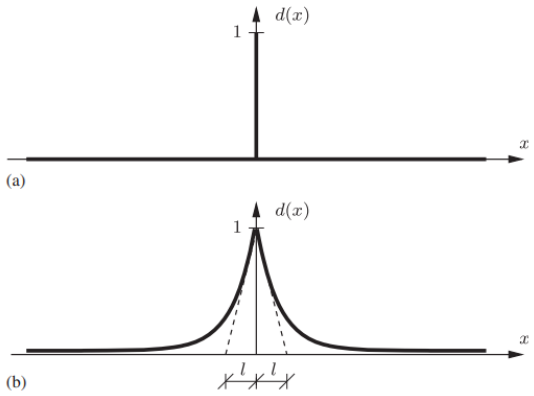

Figure 21: Sharp crack geometry, and the diffuse representation of the crack with length scale ℓ. This figure is borrowed from this paper.

We have claimed that the energy associated with the opening of cracks in a homogeneous material (constant fracture energy G) is

$$\mathcal{E}_\phi = \frac{G}{2\ell}\int \phi^2 + \ell^2 \frac{\partial \phi}{\partial x_i}\frac{\partial \phi}{\partial x_i} d\Omega$$

The material parameter G measures the energy required to open a unit surface area of crack, meaning that it has units J/m^2. The total energy expended in opening cracks is then $G\Gamma$ where Γ is the total area of cracks formed. This implies that for a given phase field ϕ, the crack area is

$$\Gamma = \frac{1}{2\ell}\int \phi^2 + \ell^2 \frac{\partial \phi}{\partial x_i}\frac{\partial \phi}{\partial x_i} d\Omega$$

It is not at all clear why this should be the case. It makes sense that the total crack area could be computed by integration the damage over the domain, but why the "density" of crack area takes this form is not obvious. We can begin to familiarize ourselves with this construction of the crack area by considering

a simple example. A sharp crack in an infinite 1D bar with cross-section A will be spread out over a finite width, as shown in Figure 21. The sharp crack is

$$\phi(x) = \begin{cases} 1 & x = 0 \\ 0 & \text{otherwise} \end{cases}$$

whereas the "smeared" crack is represented by

$$\phi(x) = e^{-|x|/\ell}$$

The length scale ℓ controls how narrow the crack is. Smaller length scales lead to sharper crack geometries. This crack shape is not based on any physics, it is simply a reasonable seeming approach to spread the crack over a finite width. Now, observe that this function satisfies the following differential equation:

$$\phi(x) - \ell^2 \frac{\partial^2 \phi}{\partial x^2} = 0, \quad \phi(0) = 1, \quad \frac{\partial \phi}{\partial x}(-\infty) = \frac{\partial \phi}{\partial x}(\infty) = 0$$

This is a bit of strange differential equation given that it has no forcing term and is driven by a prescribed value, which would need to be enforced as a constraint. The calculus of variations can be used to verify that this differential equation arises from a variational principle stated as

$$I(\phi) = \frac{A}{2} \int_{-\infty}^{\infty} \phi^2 + \ell^2 \left(\frac{\partial \phi}{\partial x} \right)^2 dx$$

The cross-sectional area appears because we integrate over the volume of the bar, but make use of fact that the phase field only depends on the axial coordinate x. The differential equation expresses the condition for a minimum of this energy-like functional. The smeared approximation of the sharp crack we have given can be conceptualized as the minimum to this energy-like functional given the constraint that $\phi(0) = 1$ and the two zero Neumann boundary conditions at $\pm\infty$. Seeing how the minima of this energy functional interpolates between the two boundary conditions and a prescribed value of the damage gives a sense of its behavior. In this case, it seems to prefer sharp gradients which quickly drive the solution down to zero. The length scale ℓ controls how localized the solution is. Note that governing equation $\phi = \ell^2 \phi''$ states that the solution equals its curvature at each point. This means that if the solution is nonzero, it must be changing rapidly in a convex manner. This helps us understand its tendency to localize.

If we take the diffuse crack $\phi = e^{-|x|/\ell}$ and plug it into the functional $I(\phi)$, one can easily show that

$$I(e^{-|x|/\ell}) = A\ell$$

Remember that we have used this diffuse crack approximation to model complete fracture of the bar. This means that, by construction, we expect

the area exposed from cracking to be the cross-sectional area A, thus the total energy expended in fracture is GA. We do not want the crack area to depend on how we smooth out the sharp crack geometry with the length scale ℓ. Thus, we can see that the value of the minimum of the new functional $\Gamma(\phi) = I(\phi)/\ell$ is simply the cross-sectional area A. From this particular example, we are led to the conclusion we hoped for, namely that the crack area is given by

$$\Gamma = \frac{1}{2\ell} \int_\Omega \phi^2 + \ell^2 \left(\frac{\partial \phi}{\partial x} \right)^2 d\Omega$$

where $\int(\cdot)d\Omega = A\int(\cdot)dx$. Now the fracture area for the fully formed crack is independent of the length scale, as desired. This is a bit of an unsatisfying argument, though. To summarize: a particular form of diffuse crack was assumed which seemed to arise as the minimum of an energy functional. This energy functional was modified slightly such that its value when evaluated at the crack was the cross-sectional area, which in this particular case was also the crack area. Is this grounds to claim that in all cases, the functional Γ takes in the phase field and approximates the crack area? It does not seem that the 1D example can be pushed any further to help answer this question. Nor does it seem like an analogous analytical example is available in 2D. Thus, we can turn to a computational example. Consider the following problem, depicted schematically in Figure 22. We have a square plate with a notch of length a. We imagine this notch as fully fractured material and that the notch is at $x_2 = L/2$, thus we have $\phi(s, L/2) = 1$ for $0 < s < a$. We then use the energy functional Γ to interpolate the damage prescribed at the notch into the entire domain of the plate. In 2D, the crack area functional is

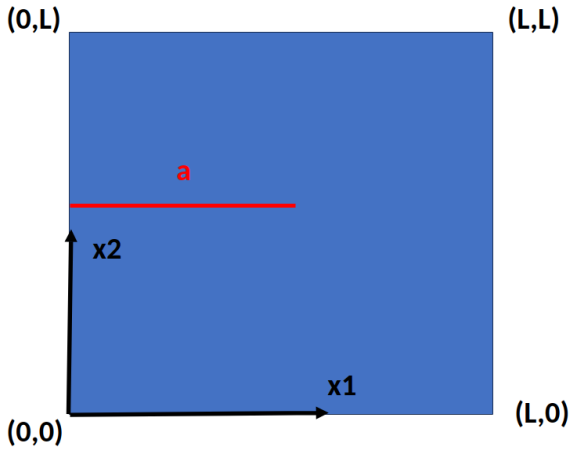

Figure 22: A square plate with side length L and a notch of length a, along which $\phi = 1$. The boundary conditions are $\frac{\partial \phi}{\partial x_i} n_i = 0$ where n is the local outward facing normal along the four edges.

$$\Gamma = \frac{1}{2\ell}\int \phi^2 + \ell^2 \frac{\partial \phi}{\partial x_i}\frac{\partial \phi}{\partial x_i} dA$$

Note that the zero Neumann boundary conditions are enforced weakly by this energy functional. We need find a phase field which minimizes this functional subject to the constraint that $\phi = 1$ along the notch. Call this solution $\tilde{\phi}$. We want to verify with a computational example that $\Gamma(\tilde{\phi}) \approx a$. In other words, we know that the crack length should be approximately the length of the notch (because we prescribed it), and we want to verify that the functional Γ really does approximate the crack length. We can discretize the phase field ϕ with a neural network, and define an objective

$$\Pi = \frac{1}{2\ell}\int \phi^2 + \ell^2 \frac{\partial \phi}{\partial x_i}\frac{\partial \phi}{\partial x_i} dA + \frac{\lambda}{2}\int_0^a \Big(\phi(s, L/2) - 1\Big)^2 ds$$

where λ is a penalty parameter used to enforce the constraint the crack is fully formed along the notch. We can compute the gradient of this with respect to the neural network parameters defining the phase field, and plug this in to an unconstrained optimization algorithm to determine the minimizer $\tilde{\phi}$. Once we have the solution for a given notch length a from solving the optimization problem, we can compute $\Gamma(\tilde{\phi})$ and compare it to the notch length. See Figures 23-25 for results. Like the 1D example, these results suggest that the crack area functional leads to localized solutions, and its value corresponds to the total crack area for a given phase field.

B Strong Form of the Phase Field Model

For completeness, we will derive the strong form of the governing equations for the total potential energy of the phase field model. Even if these equations are not used in a numerical implementation, they do provide some additional insight into the mechanics of the model. The total potential for the anisotropic phase field model is

$$\Pi = \int_\Omega (\phi - 1)^2 \Psi^+\left(\frac{\partial \underline{u}}{\partial \underline{x}}\right) + \Psi^-\left(\frac{\partial \underline{u}}{\partial \underline{x}}\right) + \frac{G}{2\ell}\left(\phi^2 + \ell^2 \frac{\partial \phi}{\partial x_i}\frac{\partial \phi}{\partial x_i}\right) d\Omega \\ - \int_\Omega b_i u_i d\Omega - \int_{\partial\Omega} t_i u_i dS$$

We ignore load stepping here for simplicity, though it is simple to factor in if one wishes to make use of the strong form. We also assume going forward that the dependence of the strain energies on the displacement gradient is implicit. The strong form of the governing equations is derived by computing the condition for a minimum of the total potential with the calculus of variations. This reads

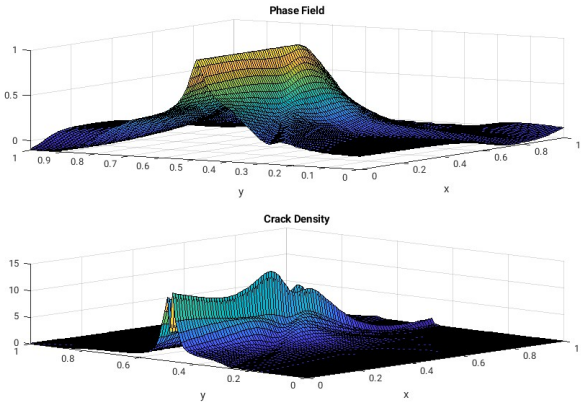

Figure 23: Surface plot of phase field and crack density in a plate with side length $L = 1$, a notch of length $a = 1/2$, and length scale of $\ell = 0.1$. The phase field interpolates the damage in the notched plate by minimizing the functional Γ. We can see that outside the crack, the phase field quickly drops to zero. The crack length is computed by evaluating Γ at the solution. For the plate with side length $L = 1$, we compute the crack length as $\Gamma = 0.7$. It makes sense that the crack length from the phase field is larger than the notch given it is smeared out over a larger region as a result of the interpolation.

$$\delta\Pi = 0 = \int 2(\phi-1)\Psi^+\delta\phi + (\phi-1)^2\frac{\partial\Psi^+}{\partial\left(\frac{\partial u_i}{\partial x_j}\right)}\frac{\partial\delta u_i}{\partial x_j} + \frac{\partial\Psi^-}{\partial\left(\frac{\partial u_i}{\partial x_j}\right)}\frac{\partial\delta u_i}{\partial x_j} + \frac{G}{\ell}\phi\delta\phi + G\ell\frac{\partial\phi}{\partial x_i}\frac{\partial\delta\phi}{\partial x_i} - b_i\delta u_i d\Omega - \int_{\partial\Omega} t_i\delta u_i dS$$

Note that the two variations δu_i and $\delta\phi$ are independent. The sets of terms they multiply must be zero independently. Grouping terms and integrating by parts the spatial gradients off the test functions, we obtain two separate integral equations

$$\int\left(\frac{\partial}{\partial x_j}\left((\phi-1)^2\frac{\partial\Psi^+}{\partial\left(\frac{\partial u_i}{\partial x_j}\right)} + \frac{\partial\Psi^-}{\partial\left(\frac{\partial u_i}{\partial x_j}\right)}\right) + b_i\right)\delta u_i d\Omega = 0$$

$$\int\left(2(\phi-1)\Psi^+ + \frac{G}{\ell}\phi - G\ell\frac{\partial^2\phi}{\partial x_i\partial x_i}\right)\delta\phi d\Omega = 0$$

As is standard in the calculus of variations, we argue that because the test functions (or variations) are arbitrary, what they multiply under the integral

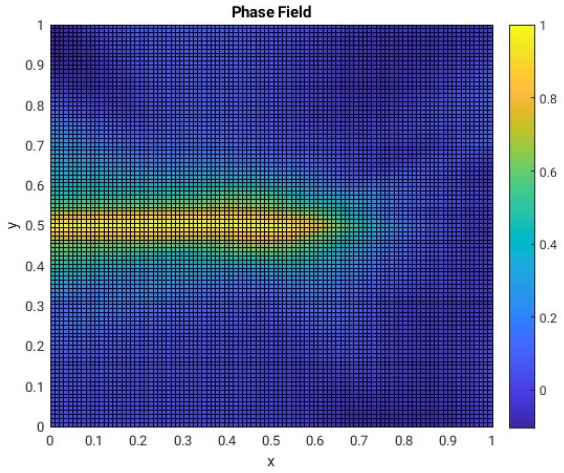

Figure 24: Heat map of the phase field computed by minimizing Γ for a notch of length $1/2$ and length scale $\ell = 0.1$. The crack area functional behaves in 2D as we expect–its minimum corresponds to sharp crack geometries, and its value corresponds to the total area of cracks formed.

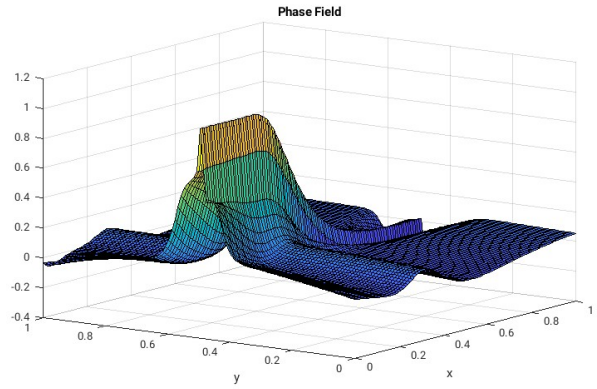

Figure 25: Phase field computed by minimizing the crack area functional for a notch of length $a = 1/4$ and length scale of $\ell = 0.05$. Evaluating Γ at this solution gives a crack area of 0.4, which again is slightly more than the notch length. This seems reasonable in light of the fact that the continuous interpolation spreads the crack over a larger region than the notch.

must be zero pointwise. This leads to the strong form of the governing equations for the anisotropic phase field problem:

$$\frac{\partial}{\partial x_j}\left((\phi-1)^2\frac{\partial \Psi^+}{\partial\left(\frac{\partial u_i}{\partial x_j}\right)}+\frac{\partial \Psi^-}{\partial\left(\frac{\partial u_i}{\partial x_j}\right)}\right)+b_i=0$$

$$\frac{G}{\ell}\left(\phi-\ell^2\frac{\partial^2\phi}{\partial x_i\partial x_i}\right)=2(1-\phi)\Psi^+$$

Remembering that derivatives of the strain energy density with respect to the displacement gradient (strain) give stresses, the first equation, which is the balance of linear momentum, says that the stress degrades with the damage, but only for the part of the strain energy associated with fracture. In other words, larger strains generate smaller stresses as the damage increases. Intuitively, this makes sense. The second equation shows that that the damage is driven by the strain energy associated with fracture, and the driving force decreases with increasing damage. It seems that the Laplacian of the damage acts as a sort of diffusive regularization to prevent the formation of zero width bands of damage. For the isotropic 1D phase field model we consider in this report, these equations read

$$\frac{\partial}{\partial x}\left((\phi-1)^2E\frac{\partial u}{\partial x}\right)+b=0$$

$$\frac{G}{\ell}\left(\phi-\ell^2\frac{\partial^2\phi}{\partial x^2}\right)=(1-\phi)E\left(\frac{\partial u}{\partial x}\right)^2$$